BRAIN COMMUNICATIONS

Kurtosis and skewness of high-frequency brain signals are altered in paediatric epilepsy

Jing Xiang,[1,2] Ellen Maue,[1,2] Yuyin Fan,[1,3] Lei Qi,[1,4] Francesco T. Mangano,[5] Hansel Greiner[2] and Jeffrey Tenney[1,2]

Intracranial studies provide solid evidence that high-frequency brain signals are a new biomarker for epilepsy. Unfortunately, epileptic (pathological) high-frequency signals can be intermingled with physiological high-frequency signals making these signals difficult to differentiate. Recent success in non-invasive detection of high-frequency brain signals opens a new avenue for distinguishing pathological from physiological high-frequency signals. The objective of the present study is to characterize pathological and physiological high-frequency signals at source levels by using kurtosis and skewness analyses. Twenty-three children with medically intractable epilepsy and age-/gender-matched healthy controls were studied using magnetoencephalography. Magnetoencephalographic data in three frequency bands, which included 2–80 Hz (the conventional low-frequency signals), 80–250 Hz (ripples) and 250–600 Hz (fast ripples), were analysed. The kurtosis and skewness of virtual electrode signals in eight brain regions, which included left/right frontal, temporal, parietal and occipital cortices, were calculated and analysed. Differences between epilepsy and controls were quantitatively compared for each cerebral lobe in each frequency band in terms of kurtosis and skewness measurements. Virtual electrode signals from clinical epileptogenic zones and brain areas outside of the epileptogenic zones were also compared with kurtosis and skewness analyses. Compared to controls, patients with epilepsy showed significant elevation in kurtosis and skewness of virtual electrode signals. The spatial and frequency patterns of the kurtosis and skewness of virtual electrode signals among the eight cerebral lobes in three frequency bands were also significantly different from that of the controls (2–80 Hz, $P < 0.001$; 80–250 Hz, $P < 0.00001$; 250–600 Hz, $P < 0.0001$). Compared to signals from non-epileptogenic zones, virtual electrode signals from epileptogenic zones showed significantly altered kurtosis and skewness ($P < 0.001$). Compared to normative data from the control group, aberrant virtual electrode signals were, for each patient, more pronounced in the epileptogenic lobes than in other lobes(kurtosis analysis of virtual electrode signals in 250–600 Hz; odds ratio = 27.9; $P < 0.0001$). The kurtosis values of virtual electrode signals in 80–250 and 250–600 Hz showed the highest sensitivity (88.23%) and specificity (89.09%) for revealing epileptogenic lobe, respectively. The combination of virtual electrode and kurtosis/skewness measurements provides a new quantitative approach to distinguishing pathological from physiological high-frequency signals for paediatric epilepsy. Non-invasive identification of pathological high-frequency signals may provide novel important information to guide clinical invasive recordings and direct surgical treatment of epilepsy.

1 MEG Center, Cincinnati Children's Hospital Medical Center, Cincinnati, OH 45229, USA
2 Division of Neurology, Cincinnati Children's Hospital Medical Center, Cincinnati, OH 45229, USA
3 Department of Pediatric Neurology, Shengjing Hospital of China Medical University, Shenyang 110004, China
4 Department of Neurosurgery, Beijing Fengtai Hospital, Beijing 100071, China
5 Division of Neurosurgery, Cincinnati Children's Hospital Medical Center, Cincinnati, OH 45229, USA

Correspondence to: Jing Xiang, MD, PhD, MEG Center, Division of Neurology,
Cincinnati Children's Hospital Medical Center, 3333 Burnet Avenue, Cincinnati, OH 45229, USA
E-mail: Jing.xiang@cchmc.org

Received October 22, 2019. Revised February 19, 2020. Accepted March 2, 2020. Advance Access publication March 31, 2020

Keywords: epilepsy; magnetoencephalography; high-frequency oscillation; epilepsy surgery; childhood epilepsy

Abbreviations: EL = epileptogenic lobe; EZ = epileptogenic zone; HFBS = high-frequency brain signal; HFO = high-frequency oscillation; MEG = magnetoencephalography; NL = normal lobe; OR = odds ratio; VE = virtual electrode

Graphical Abstract

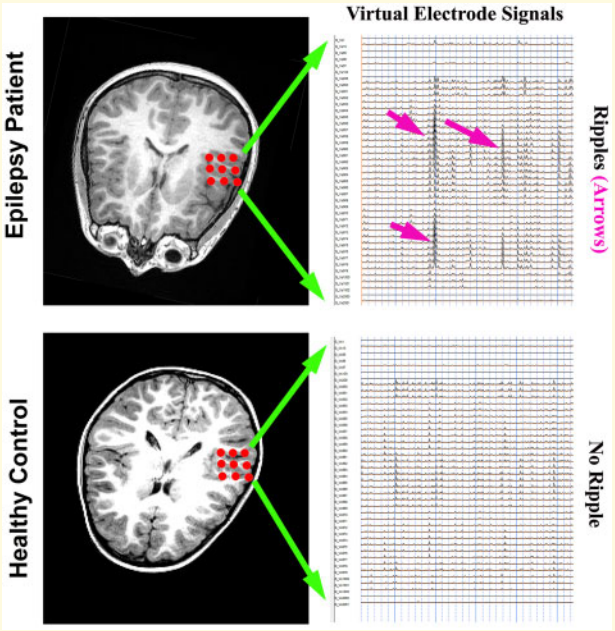

Introduction

There is solid evidence that high-frequency brain signals (HFBSs > 80 Hz) play a key role in epilepsy (Bragin *et al.*, 2011; Engel and Lopes da Silva, 2012; Worrell *et al.*, 2012). HFBS can be divided into high gamma oscillations (80–150 Hz), ripples (80–250 Hz), fast ripples (250–600 Hz) and very high-frequency oscillations (HFOs > 600 Hz) (Zijlmans *et al.*, 2012; Brázdil *et al.*, 2017; Řehulka *et al.*, 2019). Though the frequency ranges vary slightly among reports, the majority of studies of HFBS in epilepsy focus on oscillatory HFBS in 80–250 Hz (ripples) and 250–600 Hz (fast ripples), which are conventionally referred as HFOs (Rampp, 2015; Lee *et al.*, 2019).

Though HFOs are a well-recognized biomarker for epilepsy research (Frauscher *et al.*, 2017), the average population data have not yet been shown to be applicable to diagnosis of a single patient (Jacobs *et al.*, 2018; King-Stephens, 2019). One barrier hindering HFOs from wide clinical applications (Engel *et al.*, 2009; Roehri and Bartolomei, 2019) is that the brain generates both epileptic (pathological) and physiological HFOs. Physiological HFOs can be divided into elicited (functional) and endogenous HFOs. Elicited HFOs have been widely studied as functional activation in the somatosensory, language and several other brain areas (Xiang *et al.*, 2001; Xiang *et al.*, 2003). Endogenous HFOs were conventionally considered to be pathological, but an increasing list of reports indicates that endogenous HFOs can be physiological (Engel *et al.*, 2009; Roehri and Bartolomei, 2019). Since there is no one criterion that can quantitatively differentiate pathological HFOs from physiological HFOs, it is difficult to use HFOs in clinical practice (Zijlmans *et al.*, 2012; Mooij *et al.*, 2017; Frauscher *et al.*, 2018; Lee *et al.*, 2019; Roehri and Bartolomei, 2019).

Advances in magnetoencephalography (MEG) (Migliorelli *et al.*, 2017; Velmurugan *et al.*, 2018; van Klink *et al.*, 2019) and scalp EEG (Kobayashi *et al.*, 2010; Kramer *et al.*, 2019) open a new window for the study of HFBS. The non-invasive nature of MEG and EEG enable the study of HFBS in both healthy subjects and patients (Xiang *et al.*, 2009*b*; Xiang *et al.*, 2010; Tamilia *et al.*, 2017). Brain signals from healthy subjects are normative (physiological) data that provide a new approach to distinguishing pathological HFOs from physiological HFOs (Xiang *et al.*, 2009*b*). Normative data may clarify the spatial variation of HFBS in the brain. For example, MEG and EEG methods, such as virtual electrodes (VE, or virtual sensors), can be used to assess brain activities at various brain areas (Oishi *et al.*, 2006; Velmurugan *et al.*, 2018; van Klink *et al.*, 2019). It has been shown that brain activities can be registered on to template MRI in common space, which can address the spatial variation and enable the direct comparison

between patients and healthy subjects (Douw *et al.*, 2018). The variation in time and amplitude can be solved by calculating the kurtosis and skewness over a sliding time window because kurtosis is a measure of the 'spikiness' (or outliers) while skewness is a measure of asymmetry of signals (Bullock *et al.*, 1997; Hall *et al.*, 2018; Quitadamo *et al.*, 2018; Mooij *et al.*, 2020).

The objective of this study is to characterize epileptogenic HFBS in children with epilepsy and healthy controls by using VE and kurtosis/skewness. The central hypothesis is that kurtosis/skewness of VEs provides a new quantitative approach to localizing epileptogenic regions. To rigorously test the hypothesis, the present study focused on a group of patients who had clinical epileptogenic zones (EZs) determined by invasive recordings and surgical outcomes. To our knowledge, no literature has characterized the kurtosis and skewness of HFBS in various brain regions in children; let alone the alteration of HFBS in children with epilepsy compared to healthy controls. The study of pathological HFBS in paediatric epilepsy is particularly important because surgery treatment of paediatric seizures can improve the quality of life and restore the normal development of brain functions (Kadish *et al.*, 2019).

Materials and methods

Patient selection

Twenty-three patients with epilepsy (aged 6–17 years, mean: 12.56 ± 3.32 years; 12 females and 11 males) were retrospectively studied. The sample size was estimated with pilot data from our previous study (Xiang *et al.*, 2001; Xiang *et al.*, 2009*a*). The inclusion criteria for patients were (i) patients with drug-resistant epilepsy; (ii) patients had well-defined and circumscribed lesions; (iii) patients underwent pre-operative evaluation and epilepsy surgery; (iv) patient had clinical EZs determined by invasive recordings and surgical outcomes (Engel Classification of Postoperative Outcome ≤ II); (v) patient had MRI scan and MEG tests; (vi) head movement during MEG recording was <5 mm; (vii) at least 120 s of MEG recordings were clean (deflections of all MEG data within 6 Picotesla (pT) after a band-pass filter of 2–80 Hz); and (viii) post-operative assessments have been obtained at least at 1 year after surgery. The control group included 23 healthy children and adolescents (aged 6–17 years, mean: 12.60 ± 3.36; 12 females and 11 males). Controls were recruited to match the epilepsy patients for age and gender and met inclusion criteria of (i) healthy without history of neurological disorder; (ii) MRI is normal. The demographic details of the patients and controls are shown in Table 1 and Supplementary Table 1, respectively. Exclusion criteria for all participants were (i) presence of an implant, such as cochlear implant devices, a pacemaker or neuro-stimulator, devices containing electrical circuitry, generating magnetic signals or having other metal that could produce visible magnetic noise in the MEG data; (ii) noticeable anxiety (expressing worry about the tests with noticeable physical trembling or sweating) and/or inability to readily communicate with personnel operating the MEG equipment. The research protocol was reviewed by the institutional review board at Cincinnati Children's Hospital Medical Center. Informed consents, formally approved by institutional review board at Cincinnati Children's Hospital Medical Center, were obtained from each subject in accordance with the Declaration of Helsinki.

MEG recording

The MEG recordings were performed in a magnetically shielded room using a whole head MEG system (VSM MedTech Systems Inc., Coquitlam, BC, Canada) in the MEG Center at Cincinnati Children's Hospital Medical Center. Before data acquisition commenced, a small coil was attached to the nasion, left and right pre-auricular points of each subject. These three coils were subsequently activated at different frequencies for measuring subjects' head positions relative to the MEG sensors. The system allowed head localization to an accuracy of 1 mm. The sampling rate of the MEG recordings for patients was 4000 Hz. All MEG data were recorded with a noise cancellation of third-order gradients. The limitation of head movement during MEG recording was 5 mm. To identify system and environmental noise, we routinely recorded one MEG data set without subject just before the MEG tests.

MRI scan

Three-dimensional magnetization-prepared rapid acquisition gradient echo sequences were obtained for all subjects with a 3-T scanner (Siemens Medical Solutions, Malvern, PA, USA). MRI scans (three-dimensional-T_1) were performed by MRI technologists. Three fiduciary points (Multi-modality Radiographic Markers, IZI Medical Products Inc., Baltimore, MD, USA) were placed in identical locations to the positions of the three coils used in the MEG recordings, which were the pre-auricular points and the nasion, to allow for an accurate co-registration of the MEG and MRI data sets. Subsequently, all anatomical landmarks digitized in the study were made identifiable in the MR images.

Data preprocessing and workflow

To blindly analyse data, MEG and MRI data from patients and healthy controls were de-identified. MEG investigators, who were blinded to clinical results, performed data processing. After excluding bad channels (e.g. continuous noise signals) and bad segments (e.g. magnetic noise from swallowing), at least two epochs of MEG data without noise were selected for following analyses.

Table 1 Clinical characteristics of patients with drug-resistant epilepsy

ID	Sex	Age	Aetiology	MRI	MEG	EEG	iEEG (ictal)	Surgery	Outcomes
1	M	13	FCD	L Hi	L TF	L T; L central	L TF	L TF	Ia
2	F	11	TSC	R F	R F	R hemisphere	R F	R F	Ia
3	M	14	FCD	L T	L T	L T	L T	L T	Ia
4	M	14	FCD	B-MTS	L TO	L hemisphere	L TO	L TO	Ia
5	F	16	TSC	Multiple tubers	L FT	L hemisphere	L FT	L FT	Ia
6	F	9	Unknown	R H	R T	Bi FT	R T	R T	Ia
7	F	16	TSC	Multiple tubers	L FT	Multi-focal	L FT	L F	II
8	F	17	TSC	Multiple tubers	Bi FT	Multi-focal	Bi FT	Bi F	II
9	M	6	Tumour	Normal	L F	L hemisphere	L F	L F	Ia
10	M	9	TSC	Multiple tubers	R FT	Bi FT	R FT	R FT	Ib
11	M	10	TSC	Multiple tubers	L FT	L FT	L FT	L FT	Ia
12	M	11	Stroke	Normal	L PO	L hemisphere	L PO	L PO	Ia
13	M	6	TSC	Multiple tubers	R FT	R FT	R FT	R FT	Ia
14	M	14	FCD	L F	L F	Bi F	L F	L F	Ia
15	M	14	Tumour	L T	L T	Bi FT	L FT	L T	Ia
16	F	16	FCD	L F	R F; L T	Bi T	L T; R F	L F	Ia
17	F	13	FCD	Normal	L F	Bi F	L F; L centre	L F	Ia
18	F	18	FCD	Normal	L T	L T	L T	L T	Ia
19	F	13	Stroke	L P	L P	L P	L P	L P	Ia
20	F	15	Cavernous angiomas	L F	L F	L FT	L F	L F	Ia
21	F	13	Trauma	Normal	R O	R hemisphere	R O	R O	Ia
22	F	8	FCD	Normal	R TO	R TPO	R TO	R T	II
23	M	13	Stroke	L P	L P	L P	L P	L P	Ia

Bi = bilateral; F = female; F = frontal; FCD = focal cortical dysplasia; Hi = hippocampal; L = left; M = male; MTS = middle temporal sclerosis; O = occipital; P = parietal; R = right; T = temporal; TSC = tuberous sclerosis.

To ensure a stable result, each epoch of data was 120 s. Once MEG data were selected, three band-pass filters were applied to analyse signals in three frequency bands, which included 2–80, 80–250 and 250–600 Hz, respectively. Since the true EZs are unknown before clinical invasive recording, we scanned epileptogenic regions by analysing VEs in eight lobes, which included left/right frontal, temporal, parietal and occipital cortices. The key comparisons and workflows are shown in Fig. 1.

Co-registration of VE and MRI

To compare VE signals from patients and controls at source levels, MEG data were overlapped onto MRI with three fiducial points (see Fig. 2 for example). The location of the VE provided the spatial information for comparing VE signals with clinical invasive recordings, which have been described in previous reports (Oishi *et al.*, 2006; van Klink *et al.*, 2017). We also segmented the co-registered MRI. We used MNI templates for group comparisons (Douw *et al.*, 2018). The spatial resolution of VEs was 6 mm. To confirm VE abnormality in epilepsy, we also compared VEs from EZ and VEs from areas out of EZ. To curtail the effect of VE variation among brain areas, we computed the minimum, mean and maximum values of groups of VEs for aforementioned eight cerebral lobes.

Computing VE signals

We used beamforming (or spatial filtering) to calculate VE signals (waveforms). The detailed mathematic algorithms have been described in previous reports (Xiang *et al.*, 2009*a*; 2014; 2015). VE signals were computed for MEG data in three frequency bands (2–80, 80–250 and 250–600 Hz). VEs in the three frequency bands were computed with the exact same setting except the band-pass filters, which were 2–80, 80–250 and 250–600 Hz, for each corresponding frequency band, respectively. Since the EZs remained unknown before invasive recordings, to blindly and objectively scan putative epileptogenic regions, we computed grid VEs for each patient. Grid VEs were a set of VEs uniformly spaced at a designated resolution (6 mm) for the entire brain. Since each VE signal was from a specific brain area within the grid, we could identify the epileptogenic regions by analysing VEs with abnormal signals. Figure 2 shows an example of brain region with abnormal VE signals (e.g. ripples, fast ripples).

Quantifying kurtosis and skewness of VE signals

After computing all VE signals, we then calculated kurtosis and skewness for each VE signal. Kurtosis was used as it was a higher-level statistic, which provided a measure of the spikiness of signals. The formula of kurtosis has been described in previous reports (Prendergast *et al.*, 2013; Quitadamo *et al.*, 2018). Skewness provided a measure of the asymmetry of intrinsic brain activity (Letham and Raij, 2011). The formula of skewness has been described in previous reports (Letham and Raij, 2011). The function of kurtosis/skewness analysis was

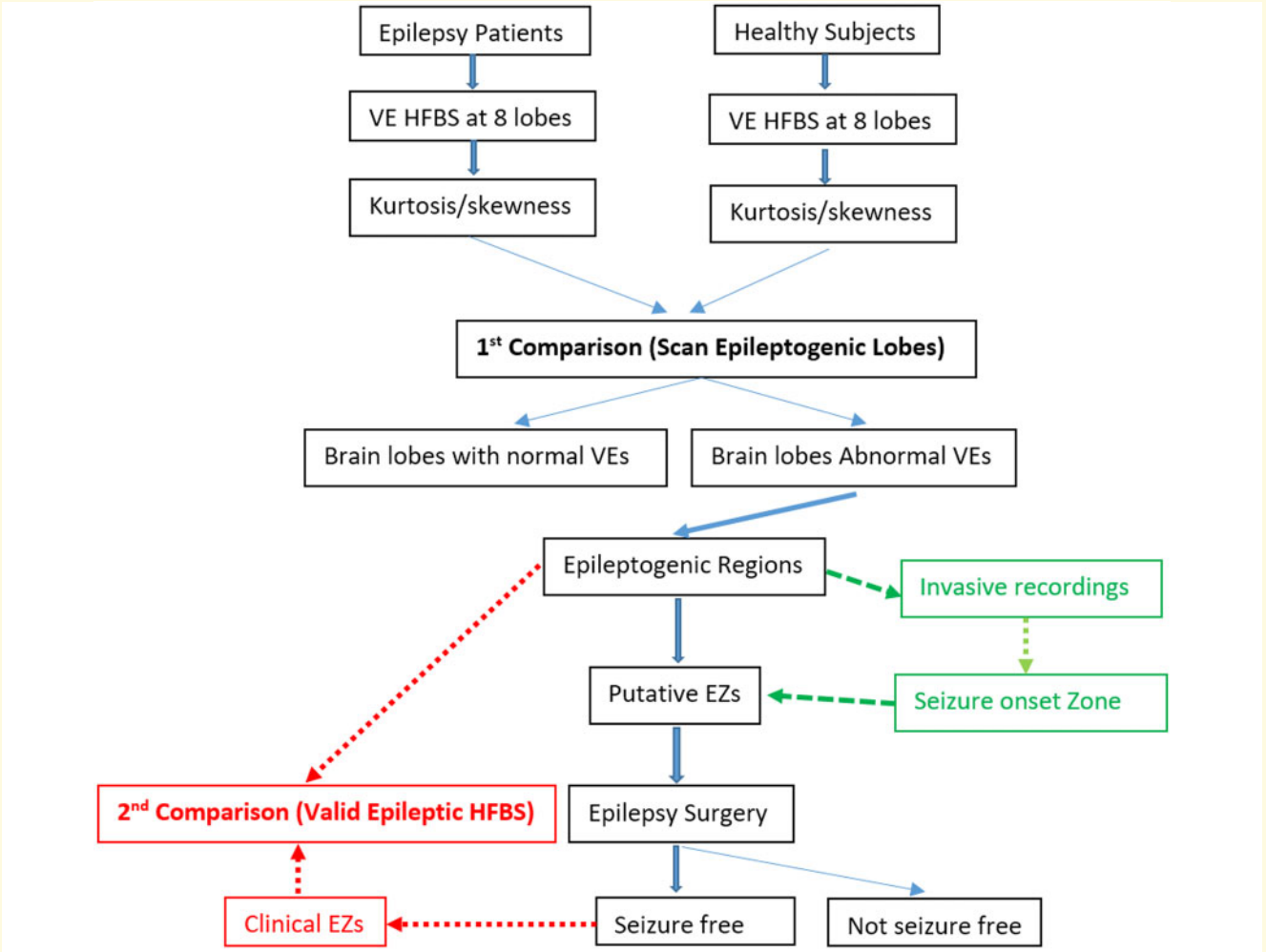

Figure 1 The workflow for analysing epileptic and epileptogenic HFBS with MEG VEs. Since the true clinical EZs are unknown before invasive recordings, we propose an objective and blind scan of epileptogenic lobes by quantitatively comparing HFBS at VEs between epilepsy patients and healthy controls (first comparison). To rigorously investigate the relationship between VE HFBS and clinical EZs, we used clinical EZs determined by invasive recordings (clinical 'gold standard') and surgical outcomes to characterize epileptogenic HFBS.

implemented in MEG Processor, a software package used in the present study. The software provided users with a versatile graphic interface and flexible, modular framework within which to analyse VE signals (Oishi *et al.*, 2006; Xiang *et al.*, 2014; Xiang *et al.*, 2015). We calculated the skewness of every VE signal in three frequency bands (2–80, 80–250 and 250–600 Hz). For group comparisons, we computed the minimum (min), mean, maximum (max) for each frequency band in each of the eight lobes for each patient and healthy subject. We reported on the distribution of the minima, means and maxima.

Clinical localization of EZ

Putative EZs in epilepsy patients were estimated by using clinical data obtained during preoperative workup and then refined with intraoperative corticography for epilepsy surgery (Greiner *et al.*, 2016). In clinical practice, non-invasive clinical data, which included clinical history, scalp EEG, MRI, positron emission tomography–computed tomography, video-EEG and MEG, were used to estimate the putative epileptogenic regions (see Fig. 1). The putative epileptogenic regions were used as the indication to perform extra-operative and intraoperative corticography. Specifically, by placing electrodes directly on (electrocorticography) or in (stereoelectroencephalography) the brain, the seizure onset zone, a surrogate of EZs, was delineated for surgical resection. To confirm EZs for each patient, we also obtained post-operative assessments at least at 1 year after surgery. Only putative EZs, whose resection resulted in free of disabling seizures or almost seizure-free (Engel Surgical Outcome Scale $\leq$ II; ILAE Outcome Scale $\leq$ 3) (Durnford *et al.*, 2011), were considered to be true EZs. Digital photos were taken before and during the operation to record the placements of the electrodes for VE analyses.

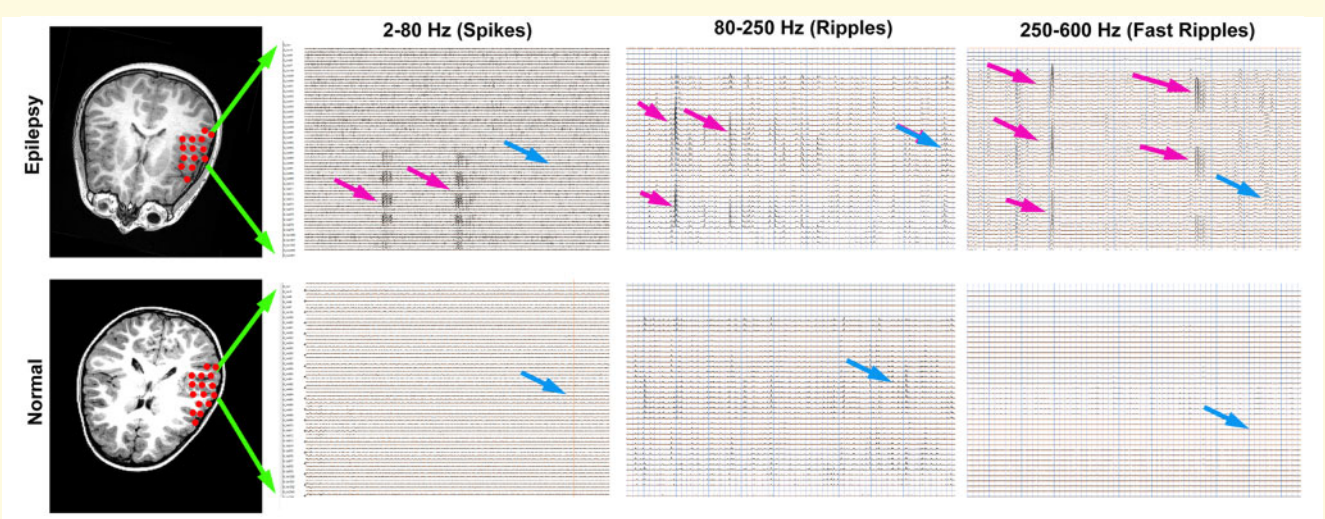

Figure 2 VE signals in 2–80 Hz, 80–250 Hz (ripples) and 250–600 Hz (fast ripples). The left column shows the location of VE (red dots), which can provide the spatial information of VEs (e.g. the left temporal lobe). The right columns show the waveforms of VE signals in three frequency bands, which enable us to analyse the kurtosis/skewness of brain activity. The top row shows VE signals from an epilepsy patient while the bottom row shows VE signals from a normal control (a healthy subject). In comparison to HFBS in the healthy subject (blue arrows), VE waveforms from the epilepsy patient showed some epileptic HFBS with elevated amplitude and kurtosis (red arrows). In comparison to epileptic HFBS, physiological HFBS have low amplitude and kurtosis (blue arrows). Due to the amplitude of physiological HFBS is low, it is difficult to visually detect the events of physiological HFBS.

Performance assessment of detection of pathological HFBS

After measuring the mean and standard deviation of kurtosis/skewness of each lobe in the control group (normative data), we used the normative mean ±3 SD as a threshold to define the abnormality of VE signals in the patient group. If the kurtosis/skewness of VE signals in a patient was out of the threshold (≥ control mean ±3 SD), the VE signals would be considered as an abnormality. Otherwise, if the kurtosis/skewness of VE signals was within the threshold, the VE signals would be considered as normal. The lobes with EZs were considered as epileptogenic lobes (ELs). The lobes without EZs were considered as normal lobes (NLs). To determine if the abnormalities in skewness and kurtosis were more pronounced in the ELs than in other regions, we calculated the odds ratio (OR) of abnormalities in lobes by dividing the odds of abnormalities in the ELs by the odds of abnormalities in the NLs (OR = odds in ELs/odds in NLs) for each frequency band. The details of the method for calculating OR have been described in a previous report (Tamhane *et al.*, 2016). By using aforementioned threshold, if VE signals with abnormal kurtosis/skewness were localized to the clinical EZs, we considered the abnormalities of these VE signals were true positive. If VE signals with abnormal kurtosis/skewness were localized to normal brain areas, which were out of the EZs, we considered these abnormalities of VE signals were false positive. If VE signals from NLs showed normal kurtosis or skewness, we considered the lack of the abnormalities of VE signals was true negative. If VE signals from the EZs showed normal kurtosis/skewness, we considered the lack of the abnormalities of VE signals was false negative. The sensitivity and specificity as the evaluation metrics were then calculated with the following equations:

$$\text{Sensitivity} = 100 \times \text{TP}/(\text{TP} + \text{FN})$$
$$\text{Specificity} = 100 \times \text{TN}/(\text{TN} + \text{FP}).$$

We analysed the sensitivity and specificity for the kurtosis/skewness of VE signals for all the three frequency bands.

Statistical analysis

The normality of all values was checked with the Kolmogorov–Smirnov test. The comparisons between patients and controls were performed using the Student's *t*-test except the measurements of skewness in 2–80 Hz, which were not normally distributed, were therefore analysed with Wilcoxon signed rank tests and independent sample Mann–Whitney U-tests for comparisons. Similarly, according the normality of data, we used the Student's *t*-test and/or Mann–Whitney U-tests to analyse the differences of VE signals between the EZs and brain areas out of the EZs. Analysis of variance (ANOVA) was used to analyse the variation of kurtosis/skewness among eight cerebral cortices and three frequency bands. The interaction between the alteration of epilepsy and age/gender were also analysed with ANOVA. The correlations of kurtosis/skewness and age were estimated with the

Spearman's rank correlation. The significance level was set at $P < 0.05$. False discovery rate correction was applied for multiple comparison (Benjamini and Hochberg, 1995) (e.g. for eight brain areas and three frequency bands, $P < 0.002$). All statistical analyses were performed in Microsoft Excel 2013, R 3.6.1 and SPSS software package version 22.0.0.0 (Armonk, NY: IBM Corp.).

Data availability

Anonymized data are available upon request. The data of the present study are one part of our research project registered at clinical trial (ClinicalTrials.gov NCT00600717). Data sharing is governed by institutional review board protocols and participants' privacy and confidentiality will be protected in accordance to Food and Drug Administration (FDA) and Health Insurance Portability and Accountability Act (HIPAA) guidelines.

Results

Characteristics of patients and controls

The demographic and clinical information of the patients are shown in Table 1. The demographic and characteristic of the control group are shown in Supplementary Table 1. MRIs from all healthy subjects were normal. There were no significant differences between the two groups of participants in terms of age and gender. Clinical pre-surgical evaluations, which included invasive recordings, revealed at least one EZ for each patient. All patients underwent epilepsy surgery and 20 out of the 23 patients had seizure freedom (see Table 1). Three of the 23 patients had multifoci and some of the foci could not be resected because the foci were adjacent to eloquent cortices. Though the postoperative outcomes of the three patients were 'almost seizure-free' (Engel Surgical Outcome Scale < II), the seizures from the resected EZs as anticipated by clinicians were completely disappeared. We, therefore, considered the resected EZs were true EZs. To provide solid results, we analysed the data with or without the three patients; only results that showed statistical significance in both conditions were reported in this study.

VE signals were significantly altered in epilepsy

Patients with epilepsy had significantly enhanced kurtosis in VE signals compared to normative controls. The details of the three types of measurements including the minimum, mean and maximum values of skewness in epilepsy and control groups are shown in Figs 3–5. The minimum kurtosis could be a negative or positive value. The mean and maximum values of kurtosis were always positive. The maximum value showed the largest standard error (or standard deviation), which indicated that the maximum value had the largest inter-individual variation. Skewness analyses revealed that patients with epilepsy had significantly altered VE signals compared to normative controls (Figs 3–5). Similar to kurtosis, the minimum values of skewness could be negative or positive. However, the mean and maximum skewness were always positive.

ANOVA analyses (two factor with replication) of kurtosis revealed significant differences between epilepsy and controls in 2–80 Hz ($F = 11.12$, $P < 0.001$), 80–250 Hz ($F = 32.2$, $P < 0.00001$) and 250–600 Hz ($F = 23.57$, $P < 0.0001$). The significance of the difference held even the age, gender and measurement types were taken as confounding factors. In addition, the significance of the difference still held by using the data from the 20 patients who were completely seizure free (see Table 1).

Abnormalities of VE signals in epilepsy were spatial dependent

The spatial patterns (distribution) of VE signals in epilepsy groups were significantly different from controls (Figs 3–5). The most significant spatial pattern of kurtosis in the epilepsy data was found in the 80–250 Hz in the maximum value. The maximum values of kurtosis in the left frontal and temporal lobes were significantly higher than that of the right occipital ($P < 0.01$). The most significant spatial pattern of skewness was found in the 250–600 Hz in the maximum value. The maximum values of the skewness in 250–600 Hz in the left frontal were significantly higher than that of the right occipital cortices ($P < 0.01$). These spatial patterns were significantly different from the controls.

ANOVA analyses revealed that there was interaction between cerebral lobes and epilepsy in 80–250 Hz in the maximum value of kurtosis ($F = 6.84$, $P < 0.05$). In addition, there was interaction between cerebral lobes and epilepsy in 250–600 Hz in minimum ($F = 7.39$, $P < 0.01$) and mean ($F = 6.93$, $P < 0.02$) values of skewness.

Abnormalities of VE signals in epilepsy were frequency specific

A comparison of VE signals in three frequency bands revealed frequency-specific abnormalities (Figs 3–5). There were significant differences between the 80–250 and 2–80 Hz in the maximum value of kurtosis in the left frontal cortex ($P < 0.001$) and left temporal cortices ($P < 0.001$) in the epilepsy group, but not in the controls. Skewness analyses of epilepsy data revealed significant differences between the 80–250 and 2–80 Hz in the maximum value of skewness in the left frontal cortex ($P < 0.001$) and left temporal cortices ($P < 0.001$).

ANOVA analyses of kurtosis measurements revealed interaction between epilepsy and frequency bands in the

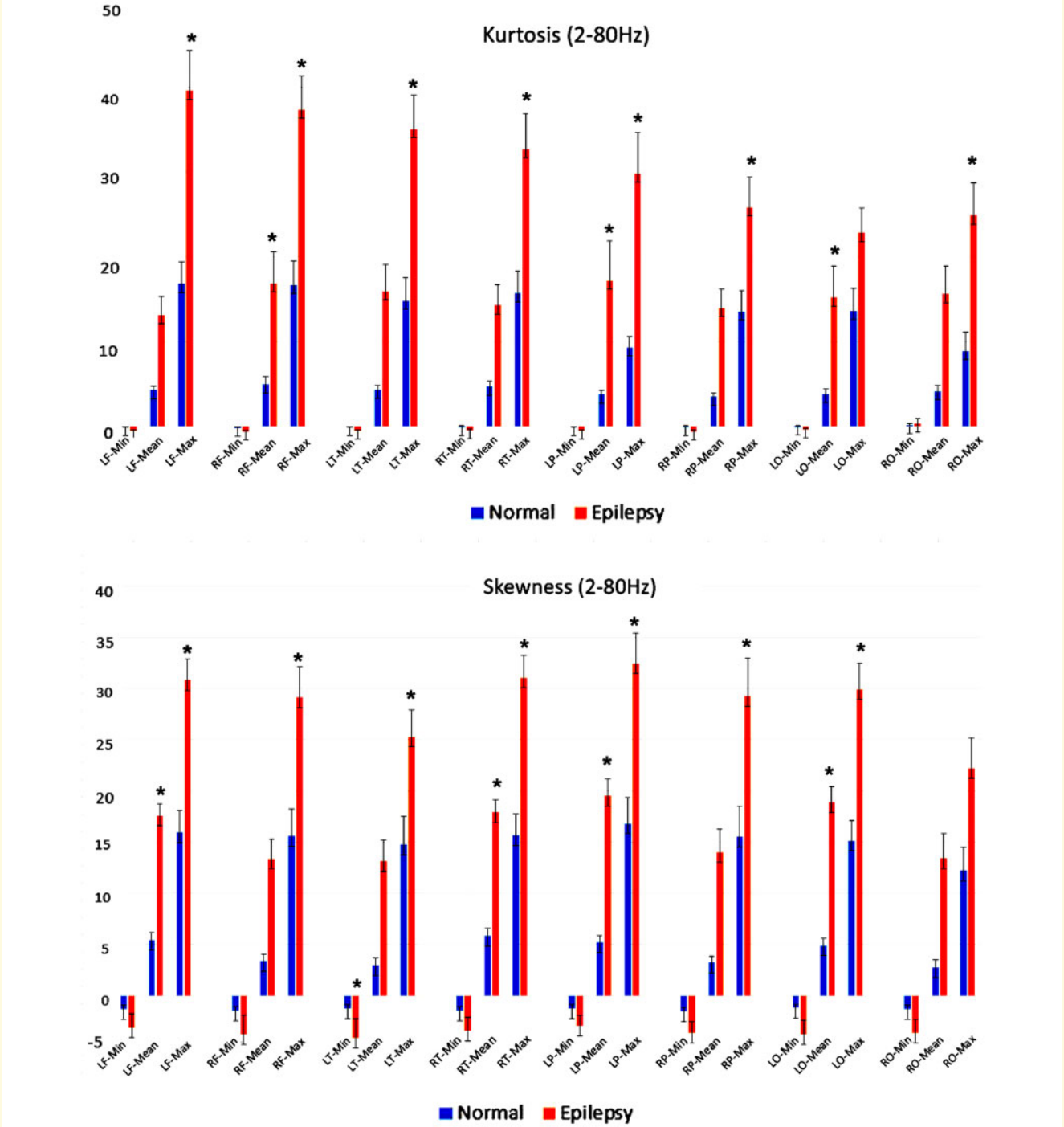

Figure 3 Column charts showing kurtosis and skewness of VE signals in 2–80 Hz. VEs in eight cerebral lobes, which include LF, RF, LT, RT, LP, RP, LO and RO lobes, are analysed. The minimum (Min), mean (Mean) and maximum (Max) values of the kurtosis/skewness in each lobe are measured, respectively. The star ('*') indicates that the difference between epilepsy (red) and normal (blue) in the corresponding measurement pair is statistically significance ($P < 0.001$). Lf = left frontal; LO = left occipital; LP = left parietal; LT = left temporal; RF = right frontal; RO = right occipital; RP = right parietal; RT = right temporal.

maximum value of kurtosis ($F = 8.91$, $P < 0.01$). In addition, there was interaction between epilepsy and frequency bands in the maximum value of skewness ($F = 7.08$, $P < 0.01$).

Kurtosis and skewness were increased in EZs

Compared to VEs from the brain areas out of the EZs, VEs from the EZs showed significantly elevated kurtosis

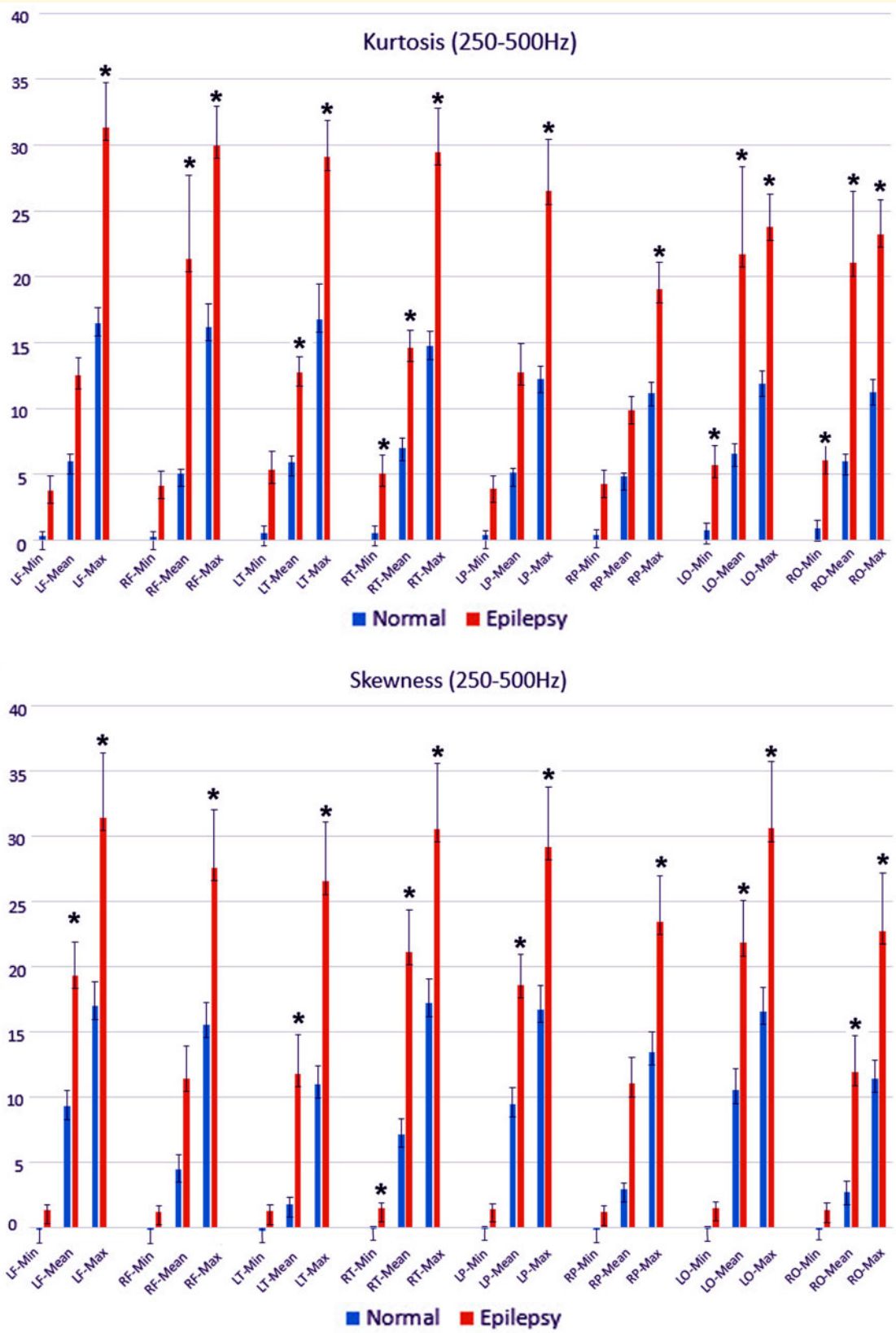

Figure 4 Column charts showing kurtosis and skewness of VE signals in 80–250 Hz. VEs in eight cerebral lobes, which include LF, RF, LT, RT, LP, RP, LO and RO lobes, are analysed. The minimum (Min), mean (Mean) and maximum (Max) values of the kurtosis/skewness in each lobe are measured, respectively. The stars indicate that the difference between epilepsy (red) and normal (blue) in the corresponding measurement pair is statistically significance (*$P < 0.001$). Lf = left frontal; LO = left occipital; LP = left parietal; LT = left temporal; RF = right frontal; RO = right occipital; RP = right parietal; RT = right temporal.

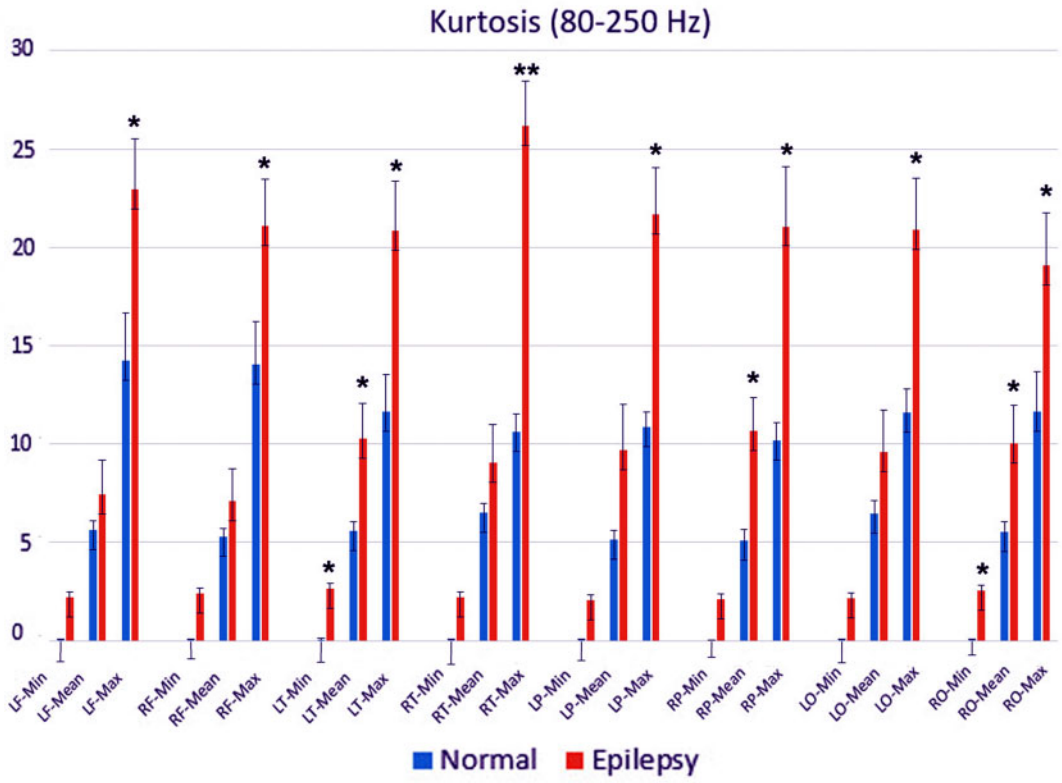

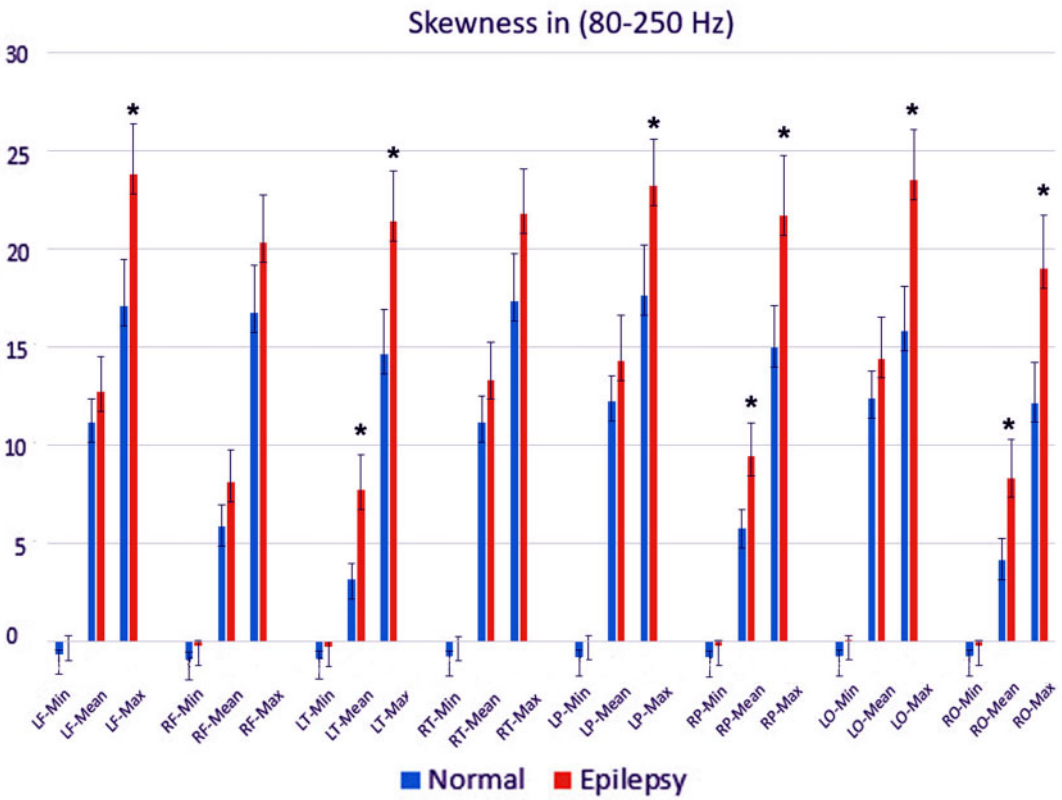

Figure 5 Column charts showing kurtosis and skewness of VE signals in 250–600 Hz. VEs in eight cerebral lobes, which include LF, RF, LT, RT, LP, RP, LO and RO lobes, are analysed. The minimum (Min), mean (Mean) and maximum (Max) values of the kurtosis/skewness in each lobe are measured, respectively. The stars indicate that the difference between epilepsy (red) and normal (blue) in the corresponding measurement pair is statistically significance (*$P < 0.001$). Lf = left frontal; LO = left occipital; LP = left parietal; LT = left temporal; RF = right frontal; RO = right occipital; RP = right parietal; RT = right temporal.

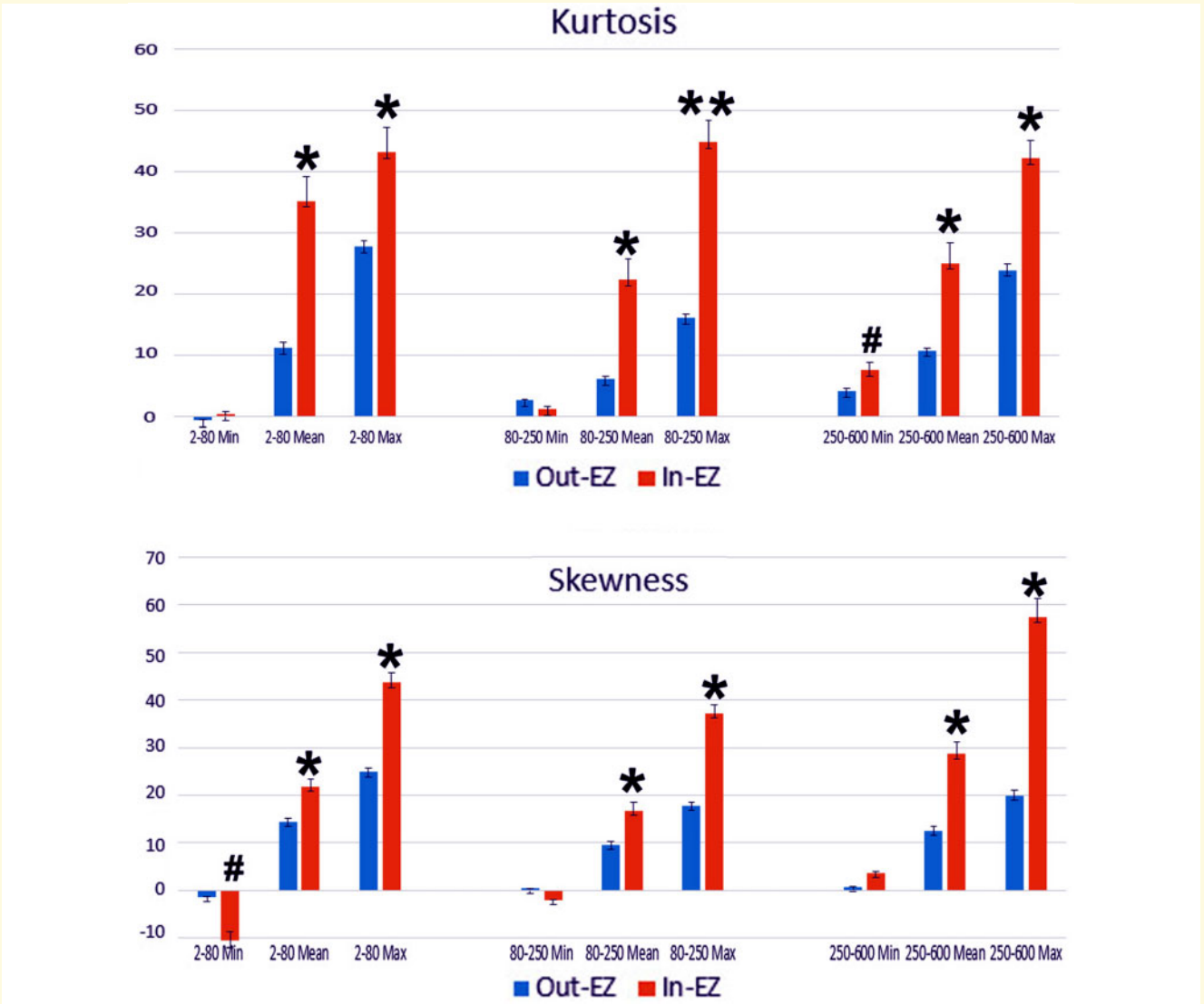

Figure 6 Column charts showing VE signals from clinical EZs and VE signals from brain areas out of clinical EZs (non-EZ). The minimum (Min), mean (Mean) and maximum (Max) values of VE signals in three frequency bands (2–80, 80–250 and 250–600Hz) are measured, respectively. The stars indicate that the difference between EZ (red) and Non-EZ (blue) in the corresponding measurement pair is statistically significance (#$P < 0.002$; *$P < 0.001$; **$P < 0.0001$).

(Fig. 6). Skewness analyses also revealed significant alteration of skewness in VE in the EZs compared to VE in the brain areas out of the EZs (Fig. 6). Different from the kurtosis, the skewness of VEs in 2–80 Hz in the EZs was predominantly negative (Fig. 6).

ANOVA analyses revealed that there was interaction between EZs and frequency bands in kurtosis ($F = 21.71$, $P < 0.0001$). There was also interaction between EZs and frequency bands in skewness ($F = 7.08$, $P < 0.01$).

Focal alteration of VE signals pointed to EZs

Analyses of the locations of VEs in the patient group showed that the total ELs (lobes with EZs) were 37; while the total NLs (lobes without EZs, NLs) were 147. The abnormalities in kurtosis and skewness were more pronounced in the ELs than in other NLs (Supplementary Table 2). Analyses of the ORs for the appearances of the abnormalities in kurtosis and skewness in cerebral lobes revealed that there were statistically significant higher ORs of abnormalities in kurtosis and skewness in the ELs than in the NLs ($P < 0.0001$). These statistical results indicated that the abnormalities in kurtosis and skewness pointed to epileptogenic regions. Using clinical EZs as the 'gold standard', the sensitivity and specificity of VE-based localization of EZs are shown in Fig. 7 (kurtosis is the up chart; skewness is the low chart). The results revealed that the highest sensitivity of kurtosis measurements was the maximum value of VE signals in 80–250 Hz, which

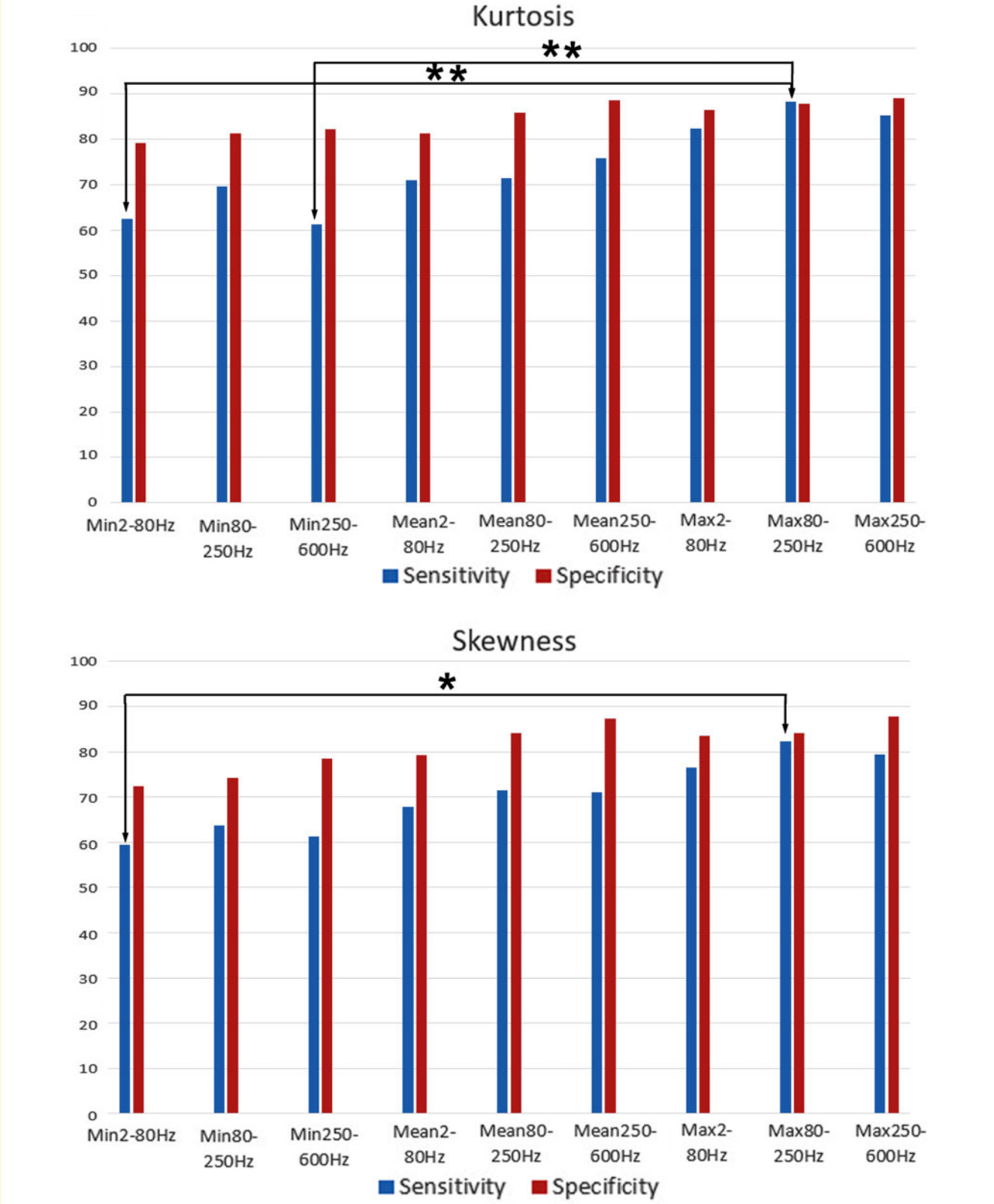

Figure 7 Column charts showing the sensitivity and specificity of localization of EZs with VEs and normative data. Epileptogenic signals are defined as the kurtosis/skewness of VE signals is beyond the mean ± 3 SD of normal data. The putative EZs are delineated with the locations of the VEs with epileptogenic signals. The true EZs are delineated with invasive recordings and surgical outcomes. The minimum (Min), mean (Mean) and maximum (Max) values of VE signals in three frequency bands (2–80, 80–250 and 250–600Hz) are used to localize EZs, respectively. The stars indicate that the difference between two corresponding measurement pair (line arrows) is statistically significance (*$P < 0.001$; **$P < 0.0005$).

was significantly higher than the minimum value in 2–80 and 80–250 Hz. The highest specificity of kurtosis measurements was the maximum value in 250–600 Hz. The highest sensitivity of skewness measurements was the maximum value of VE signals in 80–250 Hz. The highest specificity of skewness measurements was the maximum value in 250–600 Hz. Kurtosis appeared to have a higher sensitivity and specificity than that of skewness, but there was no statistical significance. From frequency point of view, the highest sensitivity was in 80–250 Hz and the lowest sensitivity was in 2–80 Hz. The highest specificity was in 250–600 Hz and the lowest specificity was in the 2–80 Hz.

Discussion

The present study has demonstrated that brain signals in patients with epilepsy are significantly altered in multiple frequency bands and high-frequency signals (80–250 and 250–600 Hz) are more specific and sensitive than that of the conventional low-frequency signals (2–80 Hz) for identification of epileptic (pathological) brain activity. If both epileptic and physiological HFOs were displayed on the same window in the same scale, the epileptic HFOs are visually identifiable but the physiological HFOs are not (see Fig. 2 for example). To our knowledge, this is the first report showing quantitative kurtosis and skewness measurements of MEG VE HFBS in eight lobes for paediatric epilepsy.

Multiplicity of differences between patients and controls

The present study provides data to support the multiplicity of differences between epilepsy patients and healthy controls. In clinical practice, the EZs are unknown before invasive recordings and surgery. Therefore, the comparison of VEs in the eight lobes between epilepsy patients and healthy controls can objectively reveal the ELs. Once the ELs are identified, the putative EZs can be delineated with the groups of VEs in the lobe. Clinicians can use the putative EZs to guide invasive recordings and surgery. From methodological point of view, the comparison between epilepsy patients and healthy controls was to narrow down the epileptogenic regions from the entire brain to one or more lobes.

The comparisons of VEs in three frequency bands between epilepsy patients and controls have revealed that HFOs in 80–250 Hz (ripples) and 250–600 Hz (fast ripples) appear independently. It seems that fast ripples are more specific or pathological. Our MEG results are consistent with invasive recordings (Zijlmans *et al.*, 2012; Brázdil *et al.*, 2017; Řehulka *et al.*, 2019). Since HFBS are very weak, invasive recordings provide necessary and convincing data about the relationship between epilepsy and HFBS (Engel and Lopes da Silva, 2012; Jacobs *et al.*, 2012). If our results could be validated, non-invasive MEG VEs might be used to guide clinical invasive recordings in the future.

Abnormalities of HFBS in epilepsy can be automatically detected and quantified

Previous reports (Xiang *et al.*, 2014; Fedele *et al.*, 2016; Migliorelli *et al.*, 2017; van Klink *et al.*, 2017; Guo *et al.*, 2018) have shown the possibility to automatically detect HFOs, which include ripples and fast ripples, by using a set of criteria, such as amplitude and number of oscillations. However, even ripples and fast ripples are detected, it is still unclear if these detected ripples or fast ripples are pathological or physiological. The analysis of kurtosis and skewness of VE signals may be a feasible way for distinguishing pathological HFBS from physiological HFBS. The findings of ripples (80–280 Hz) and fast ripples (250–600 Hz) in epilepsy have drawn a great attention from the researchers. In comparison to previous reports (Zijlmans *et al.*, 2012; Mooij *et al.*, 2017; Frauscher *et al.*, 2018; Lee *et al.*, 2019; Roehri and Bartolomei, 2019), the major novel finding is the quantitative measurements of kurtosis and skewness of VE signals in epilepsy. Though additional verification and validation are necessary, building on the present study, we consider it is possible to determine the abnormalities of HFBS by measuring the kurtosis and skewness of signals. Since the abnormalities of VE signals were determined by using normative data, this approach is objective, quantitative and effective (no visual identification is necessary), which is significantly different from the conventional visual identification, which can be subjective and tedious and error-prone.

Epileptic VE signals are frequency specific

The results of VE signals in 2–80, 80–250 and 250–600 Hz indicate VE signals in 250–600 Hz had the highest specificity in the localization of EZs, which was significantly higher than that of VE signals in 2–80 Hz. This observation suggests that fast ripples in 250–600 Hz were pathological or epileptogenic signals. On the other hand, VE signals in 2–80 Hz may include more physiological or irritative brain signals that might be elevated in secondary epileptic areas. Our observation is strongly supported by previous reports (Tamilia *et al.*, 2018; Schonberger *et al.*, 2019), which have found that the resection of brain areas generating HFOs is associated with good outcomes of epilepsy surgery (Tamilia *et al.*, 2018).

The results of two frequency bands of HFBS indicate that the measurements of VE signals in 80–250 Hz showed the highest sensitivity in localizing EZs. In comparison to VE signals in 250–600 Hz, VE signals in

80–250 Hz are typically much stronger (higher amplitude), consequently, these signals are more easily picked up by MEG. VE signals in 2–80 Hz can be stronger than that of VE signals in 80–250 Hz, however, VE signals in 2–80 Hz are not highly localized to EZs. In other words, VE signals in 2–80 Hz include more physiological signals.

Abnormalities in kurtosis and skewness are pronounced in the ELs

The results of the present study have demonstrated that there were significant differences between epilepsy and healthy control in terms of kurtosis and skewness in 2–80, 80–250 and 250–600 Hz. The significance of the difference held even the age, gender and frequency bands were taken as confounding factors in ANOVA. We have noted that the location of EZs might vary significantly among patients, due to epilepsy patients are a heterogeneous group of patients. The comparisons of VE data from these heterogeneous patients and normative data yielded heterogeneous results, which provided limited information for localizing EZs at individual levels. In other words, spatial variation of VE signals diminished the usefulness of group comparisons for localization of EZs. To facilitate the localization of EZs with normative data, we tried to compare individual patient's data to normative data in eight lobes. We have noted that the cerebral lobes in epilepsy patients with elevated kurtosis/skewness values ($\geq$ normative mean ± 3 SD) had a significantly high probability of having the EZs (high OR). The results indicate that abnormalities in kurtosis/skewness pronounced in ELs (see Supplementary Table 2). Methodologically, the comparisons of individual patient to normal controls enabled us to narrow down the epileptogenic regions from the entire brain to ELs. For research purposes, we compared the ELs estimated by VEs and the true EZs determined by clinical data; the results have confirmed that VEs with elevated kurtosis are highly localized to the EZs. Taken together, our results suggest that ELs estimated by VEs, which is based on non-invasive MEG, shall be used to guide invasive recordings and surgery in the future.

We also noted the spatial variation of kurtosis in healthy subjects in various brain regions. It has been shown that intrinsic HFBSs can be detected by MEG (Xiang *et al.*, 2009*b*), and the slightly higher kurtosis in VE signals in healthy subjects may reflect functional intrinsic activity. This observation is consistent with previous reports (Xiang *et al.*, 2001; Xiang *et al.*, 2009*a*).

Kurtosis and skewness characterize different aspects of brain activities

The results of kurtosis and skewness have showed some similarities and differences in VE signals. The kurtosis of VE signals mainly measures the 'spikiness' of brain activity while the skewness of VE signals mainly measures the symmetry of brain activity (Bullock *et al.*, 1997; Hall *et al.*, 2018; Quitadamo *et al.*, 2018). The data of the present study indicate that both kurtosis and skewness of brain activities in epilepsy were significantly altered as compared to normal controls. In comparison to previous reports (Bullock *et al.*, 1997; Hall *et al.*, 2018; Quitadamo *et al.*, 2018), one of the major innovations of the present study is the analysis of brain activity at source levels, instead of at sensor levels. Of note, the findings of abnormal kurtosis and skewness of low-frequency signals (2–80 Hz) in epilepsy are consistent with previously findings (Bullock *et al.*, 1997; Hall *et al.*, 2018; Quitadamo *et al.*, 2018).

The difference between physiological and pathological (epileptic) HFOs in terms of kurtosis is probably that the former reflect summated inhibitory postsynaptic potentials, while the latter reflect summated action potentials of synchronously bursting neurons (Bragin *et al.*, 1999; Jefferys *et al.*, 2012). Since pathological HFOs are from epileptic hypersynchronous population spikes of bursting pyramidal neurons, it is reasonable to postulate that the kurtosis/skewness of pathological HFOs, which reflects the spikiness/asymmetry of brain activities, would be elevated. Of note, our observation of increased spikiness/asymmetry in MEG data strongly supports the hypothesis proposed in previous reports (Bragin *et al.*, 1999; Jefferys *et al.*, 2012).

Limitations of the present study

To rigorously investigate the usefulness of HFOs in localization of EZs, the present study focused on a group of patients with well-defined superficial epileptic lesions, who underwent invasive recordings (clinical 'gold standard') and surgery. Consequently, the results of epilepsy surgery in these patients appeared to be very good. Of note, the results may not be able to apply to all epilepsy patients at individual levels. Specifically, some epilepsy patients may have lesions in the deep brain regions. MEG is considered to be sensitive to brain signals from the superficial, it remains unknown if our approach can localize EZs in the deep brain areas (e.g. the hippocampus).

Conclusions

Paediatric epilepsy is associated with significant alteration of VE HFBS compared to normal controls in terms of kurtosis and skewness. The alteration of VE HFBS is frequency specific. The kurtosis of VE signals in 80–250 Hz are the most sensitive biomarker while kurtosis of VE signals in 250–600 Hz are the most specific biomarker for localization of EZs. For a particular patient with epilepsy, we propose to use the maximum kurtosis in 80–250 Hz

for pre-surgical evaluation of epilepsy surgery (Phase I), and use the maximum kurtosis in 250–600 Hz for guiding invasive recordings (Phase II) in the future.

Supplementary material

Supplementary material is available at *Brain Communications* online.

Acknowledgements

The authors would like to thank Drs Douglas Rose, Hisako Fujiwara and Nat Hemasilpin for MEG data acquisition and Drs Kimberly Leiken, Yingying Wang and Kendall O'Brien for MRI scan.

Funding

The project described was supported by National Institute of Neurological Disorders and Stroke (NINDS) (R21 NS104459), the National Institutes of Health (NIH). The normative database used in the present study was partially supported by NINDS/NIH (R21NS081420, R21NS072817). This project described was partially supported by funding from the State of Ohio, Ohio Development Services Agency, Ohio Third Frontier (TECG20170361, TECG20190159). The software used in the project described was partially supported by Cincinnati Children's Hospital Medical Center's Innovation Fund.

Competing interests

The authors report no competing interests.

References

Benjamini Y, Hochberg Y. Controlling the false discovery rate—a practical and powerful approach to multiple testing. J Roy Stat Soc B Met 1995; 57: 289–300.

Bragin A, Benassi SK, Kheiri F, Engel J Jr. Further evidence that pathologic high-frequency oscillations are bursts of population spikes derived from recordings of identified cells in dentate gyrus. Epilepsia 2011; 52: 45–52.

Bragin A, Engel J, Wilson CL, Fried I, BuzsaKi G. High-frequency oscillations in human brain. Hippocampus 1999; 9: 137–42.

Brázdil M, Pail M, Halámek J, Pleinger F, Cimbálník J, Roman R, et al. Very high-frequency oscillations: novel biomarkers of the epileptogenic zone. Ann Neurol 2017; 82: 299–310.

Bullock TH, Achimowicz JZ, Duckrow RB, Spencer SS, Iragui-Madoz VJ. Bicoherence of intracranial EEG in sleep, wakefulness and seizures. Electroencephalogr Clin Neurophysiol 1997; 103: 661–78.

Douw L, Nieboer D, Stam CJ, Tewarie P, Hillebrand A. Consistency of magnetoencephalographic functional connectivity and network reconstruction using a template versus native MRI for co-registration. Hum Brain Mapp 2018; 39: 104–19.

Durnford AJ, Rodgers W, Kirkham FJ, Mullee MA, Whitney A, Prevett M, et al. Very good inter-rater reliability of Engel and ILAE epilepsy surgery outcome classifications in a series of 76 patients. Seizure 2011; 20: 809–12.

Engel J Jr, Bragin A, Staba R, Mody I. High-frequency oscillations: what is normal and what is not? Epilepsia 2009; 50: 598–604.

Engel J Jr, Lopes da Silva FL. High-frequency oscillations - where we are and where we need to go. Prog Neurobiol 2012; 98: 316–8.

Fedele T, van't Klooster M, Burnos S, Zweiphenning W, van Klink N, Leijten F, et al. Automatic detection of high frequency oscillations during epilepsy surgery predicts seizure outcome. Clin Neurophysiol 2016; 127: 3066–74.

Frauscher B, Bartolomei F, Kobayashi K, Cimbalnik J, van't Klooster MA, Rampp S, et al. High-frequency oscillations: the state of clinical research. Epilepsia 2017; 58: 1316–29.

Frauscher B, von Ellenrieder N, Zelmann R, Rogers C, Nguyen DK, Kahane P, et al. High-frequency oscillations in the normal human brain. Ann Neurol 2018; 84: 374–85.

Greiner HM, Horn PS, Tenney JR, Arya R, Jain SV, Holland KD, et al. Preresection intraoperative electrocorticography (ECoG) abnormalities predict seizure-onset zone and outcome in pediatric epilepsy surgery. Epilepsia 2016; 57: 582–9.

Guo J, Yang K, Liu H, Yin C, Xiang J, Li H, et al. A stacked sparse autoencoder-based detector for automatic identification of neuromagnetic high frequency oscillations in epilepsy. IEEE Trans Med Imaging 2018; 37: 2474–82.

Hall MBH, Nissen IA, van Straaten ECW, Furlong PL, Witton C, Foley E, et al. An evaluation of kurtosis beamforming in magnetoencephalography to localize the epileptogenic zone in drug resistant epilepsy patients. Clin Neurophysiol 2018; 129: 1221–9.

Jacobs J, Staba R, Asano E, Otsubo H, Wu JY, Zijlmans M, et al. High-frequency oscillations (HFOs) in clinical epilepsy. Prog Neurobiol 2012; 98: 302–15.

Jacobs J, Wu JY, Perucca P, Zelmann R, Mader M, Dubeau F, et al. Removing high-frequency oscillations: a prospective multicenter study on seizure outcome. Neurology 2018; 91: e1040–e52.

Jefferys JG, Menendez de la Prida L, Wendling F, Bragin A, Avoli M, Timofeev I, et al. Mechanisms of physiological and epileptic HFO generation. Prog Neurobiol 2012; 98: 250–64.

Kadish NE, Bast T, Reuner G, Wagner K, Mayer H, Schubert-Bast S, et al. Epilepsy surgery in the first 3 years of life: predictors of seizure freedom and cognitive development. Neurosurgery 2019; 84: E368–77.

King-Stephens D. The ambiguous nature of fast ripples in epilepsy surgery. Epilepsy Curr 2019; 19: 91–2.

Kobayashi K, Watanabe Y, Inoue T, Oka M, Yoshinaga H, Ohtsuka Y. Scalp-recorded high-frequency oscillations in childhood sleep-induced electrical status epilepticus. Epilepsia 2010; 51: 2190–4.

Kramer MA, Ostrowski LM, Song DY, Thorn EL, Stoyell SM, Parnes M, et al. Scalp recorded spike ripples predict seizure risk in childhood epilepsy better than spikes. Brain 2019; 142: 1296–309.

Lee S, Issa NP, Rose S, Tao JX, Warnke PC, Towle VL, et al. DC shifts, high frequency oscillations, ripples and fast ripples in relation to the seizure onset zone. Seizure 2019;

Letham B, Raij T. Statistically robust measurement of evoked response onset latencies. J Neurosci Methods 2011; 194: 374–9.

Migliorelli C, Alonso JF, Romero S, Nowak R, Russi A, Mananas MA. Automated detection of epileptic ripples in MEG using beamformer-based virtual sensors. J Neural Eng 2017; 14: 046013.

Mooij AH, Frauscher B, Gotman J, Huiskamp G. A skew-based method for identifying intracranial EEG channels with epileptic activity without detecting spikes, ripples, or fast ripples. Clin Neurophysiol 2020; 131: 183–92.

Mooij AH, Raijmann R, Jansen FE, Braun KPJ, Zijlmans M. Physiological ripples (±100 Hz) in spike-free scalp EEGs of children with and without epilepsy. Brain Topogr 2017; 30: 739–46.

Oishi M, Otsubo H, Iida K, Suyama Y, Ochi A, Weiss SK, et al. Preoperative simulation of intracerebral epileptiform discharges: synthetic aperture magnetometry virtual sensor analysis of interictal magnetoencephalography data. J Neurosurg 2006; 105: 41–9.

Prendergast G, Green GG, Hymers M. A robust implementation of a kurtosis beamformer for the accurate identification of epileptogenic foci. Clin Neurophysiol 2013; 124: 658–66.

Quitadamo LR, Mai R, Gozzo F, Pelliccia V, Cardinale F, Seri S. Kurtosis-based detection of intracranial high-frequency oscillations for the identification of the seizure onset zone. Int J Neur Syst 2018; 28: 1850001.

Rampp S. Direct current shifts, high frequency oscillations and the epileptogenic zone. Clin Neurophysiol 2015; 126: 2–4.

Řehulka P, Cimbálník J, Pail M, Chrastina J, Hermanová M, Brázdil M. Hippocampal high frequency oscillations in unilateral and bilateral mesial temporal lobe epilepsy. Clin Neurophysiol 2019; 130: 1151–9.

Roehri N, Bartolomei F. Are high-frequency oscillations better biomarkers of the epileptogenic zone than spikes? Curr Opin Neurol 2019; 32: 213–9.

Schonberger J, Frauscher B, von Ellenrieder N, Avoli M, Dubeau F, Gotman J. Fast ripple analysis in human mesial temporal lobe epilepsy suggests two different seizure-generating mechanisms. Neurobiol Dis 2019; 127: 374–81.

Tamhane AR, Westfall AO, Burkholder GA, Cutter GR. Prevalence odds ratio versus prevalence ratio: choice comes with consequences. Stat Med 2016; 35: 5730–5.

Tamilia E, Madsen JR, Grant PE, Pearl PL, Papadelis C. Current and emerging potential of magnetoencephalography in the detection and localization of high-frequency oscillations in epilepsy. Front Neurol 2017; 8: 14.

Tamilia E, Park E-H, Percivati S, Bolton J, Taffoni F, Peters JM, et al. Surgical resection of ripple onset predicts outcome in pediatric epilepsy. Ann Neurol 2018; 84: 331–46.

van Klink N, Mooij A, Huiskamp G, Ferrier C, Braun K, Hillebrand A, et al. Simultaneous MEG and EEG to detect ripples in people with focal epilepsy. Clin Neurophysiol 2019; 130: 1175–83.

van Klink N, van Rosmalen F, Nenonen J, Burnos S, Helle L, Taulu S, et al. Automatic detection and visualisation of MEG ripple oscillations in epilepsy. NeuroImage Clinical 2017; 15: 689–701.

Velmurugan J, Nagarajan SS, Mariyappa N, Ravi SG, Thennarasu K, Mundlamuri RC, et al. Magnetoencephalographic imaging of ictal high-frequency oscillations (80-200 Hz) in pharmacologically resistant focal epilepsy. Epilepsia 2018; 59: 190–202.

Worrell GA, Jerbi K, Kobayashi K, Lina JM, Zelmann R, Le Van Quyen M. Recording and analysis techniques for high-frequency oscillations. Prog Neurobiol 2012; 98: 265–78.

Xiang J, Holowka S, Sharma R, Hunjan A, Otsubo H, Chuang S. Volumetric localization of somatosensory cortex in children using synthetic aperture magnetometry. Ped Radiol 2003; 33: 321–7.

Xiang J, Korman A, Samarasinghe KM, Wang X, Zhang F, Qiao H, et al. Volumetric imaging of brain activity with spatial-frequency decoding of neuromagnetic signals. J Neurosci Methods 2015; 239: 114–28.

Xiang J, Liu Y, Wang Y, Kirtman EG, Kotecha R, Chen Y, et al. Frequency and spatial characteristics of high-frequency neuromagnetic signals in childhood epilepsy. Epileptic Disord 2009a; 11: 113–25.

Xiang J, Liu Y, Wang Y, Kotecha R, Kirtman EG, Chen Y, et al. Neuromagnetic correlates of developmental changes in endogenous high-frequency brain oscillations in children: a wavelet-based beamformer study. Brain Res 2009b; 1274: 28–39.

Xiang J, Luo Q, Kotecha R, Korman A, Zhang F, Luo H, et al. Accumulated source imaging of brain activity with both low and high-frequency neuromagnetic signals. Front Neuroinform 2014; 8: 57.

Xiang J, Wang Y, Chen Y, Liu Y, Kotecha R, Huo X, et al. Noninvasive localization of epileptogenic zones with ictal high-frequency neuromagnetic signals. J Neurosurg Pediatr 2010; 5: 113–22.

Xiang J, Wilson D, Otsubo H, Ishii R, Chuang S. Neuromagnetic spectral distribution of implicit processing of words. Neuroreport 2001; 12: 3923–7.

Zijlmans M, Jiruska P, Zelmann R, Leijten FS, Jefferys JG, Gotman J. High-frequency oscillations as a new biomarker in epilepsy. Ann Neurol 2012; 71: 169–78.